Sol–Gel Synthesis of Dodecyltrimethylammonium-Expanded Zirconium Phosphate and Its Application to the Preparation of Acidic Porous Oligomeric Gallium(III)-Exchanged Materials

ARTICLE *in* LANGMUIR · MAY 1997

Impact Factor: 4.46 · DOI: 10.1021/la961073s

Sol−Gel Synthesis of Dodecyltrimethylammonium-Expanded Zirconium Phosphate and Its Application to the Preparation of Acidic Porous Oligomeric Gallium(III)-Exchanged Materials

José Jiménez-Jiménez, Pedro Maireles-Torres, Pascual Olivera-Pastor, Enrique Rodríguez-Castellón, and Antonio Jiménez-López*

Departamento de Química Inorgánica, Cristalografía y Mineralogía, Facultad de Ciencias, Universidad de Málaga, Campus de Teatinos, 29071-Málaga, Spain

Received November 5, 1996. In Final Form: February 11, 1997[⊗]

A new sol−gel method for the direct synthesis of layered surfactant-expanded zirconium phosphates has been developed by reacting together dodecyltrimethylammonium bromide, orthophosphoric acid (85%), and zirconium tetra-*n*-propoxide in 1-propanol solution at room temperature. The resulting intercalation compounds have been characterized, and their use as starting materials for preparing gallium-containing porous solids has been evaluated. Surfactant species form a closely packed bilayer inside the phosphate interlayer region with a basal spacing of 33 Å. Gallium oligomeric species have been inserted into the host structure by ion exchange with dodecyltrimethylammonium ions. Upon calcination at 673 K, highly porous gallium(III)−zirconium phosphate composites were formed with Brunauer−Emmett−Teller surface areas between 295 and 366 $m^2\ g^{-1}$ and narrow pore size distributions. Standard techniques such as thermal programmed desorption of ammonia and pyridine adsorption have revealed their acid nature. These materials show high catalytic activity for the reaction of isopropyl alcohol decomposition at 473 K with conversions and selectivities toward propene nearly 100%.

Introduction

The continuous demand of acid solids with specific uses in catalysis and sorption has led to the development of different kinds of materials with engineered pore sizes and shapes. The best known materials are natural and synthetic zeolites, which have a widespread application in many catalytic reactions by their shape-selective characteristics.[1]

Another methodology investigated for producing acid solids with controlled porosity consists of the insertion of metal oxide nanoparticles into layered hosts, such as clays, metal(IV) phosphates, perovskites, double hydroxides, etc.[2] Although with less uniform textural characteristics than those of zeolites, some pillared layered structures show high thermal stabilities and interesting catalytic properties. Thus, pillared clays have been successfully employed in reactions such as gas oil cracking to yield gasoline under moderate conditions, disproportionation processes, alkylation of toluene, and many others.[3]

Apart from pillared clays, the preparation and properties of pillared layered phosphates, basically based on α-zirconium phosphate, $Zr(HPO_4)_2{\cdot}H_2O$, as host matrix, have been extensively studied. Covalently bonded organic species and inorganic polyoxocations have been used as the pillaring agent.[4−7] Most of the inorganically pillared phosphates are of acid nature with surface characteristics mainly determined by the type of pillaring solution utilized and the linkage established between the interlayer metal oxide and the phosphate layer, formed upon calcination. In addition to their catalytic properties,[8] these materials may be used for encapsulating nanoparticles of semiconductors,[9] for polymerization reactions of organic monomers,[10] as ion exchangers,[11] and as sensors.[12]

In spite of the considerable effort devoted to the design of porous materials, exploring new experimental routes is necessary in order to have a great variety of solids suitable for each particular application. Very recently, a new family of hybrid organo-inorganic solids, designated as MCM-type materials, has been reported,[13] in which surfactant species act as structuring agents and control fundamental characteristics such as the pore size and the stability of the resulting products. In addition to tridimensional compounds,[13] lamellar phases, e.g. layered Zn

[⊗] Abstract published in *Advance ACS Abstracts,* April 1, 1997.

(1) Corma, A. *Chem. Rev.* **1995**, *95*, 559.

(2) (a) Pinnavaia, T. J. *Science* **1983**, *220*, 365. (b) Figueras, F. *Catal. Rev.-Sci. Eng.* **1988**, *30*, 457. (c) *Pillared Layered Structures: Current Trends and Applications*; Mitchell, I. V., Ed.; Elsevier Applied Science: London, 1990. (d) Clearfield, A. In *Multifunctional Mesoporous Inorganic Solids*; Sequeira, C. A. C., Hudson, M. J., Eds.; NATO ASI, Kluwer Academic: Dordrecht, Germany, 1993, *400*, 159−178.

(3) Burch, R., Ed. *Catal. Today* **1988**, *2*, 1−185.

(4) Clearfield, A. *Comments Inorg. Chem.* **1990**, *10*, 83.

(5) Alberti, G.; Murcia-Mascarós, S.; Vivani, R. *Mater. Sci. Forum* **1994**, *152−153*, 87.

(6) (a) Clearfield, A.; Roberts, B. D. *Inorg. Chem.* **1988**, *27*, 3237. (b) Li, L.-S.; Liu, X.-S.; Ge, Y.; Li, L.; Klinowski, J. *J. Phys. Chem.* **1991**, *95*, 5910.

(7) Olivera-Pastor, P.; Maireles-Torres, P.; Rodríguez-Castellón, E.; Jiménez-López, A.; Cassagneau, T.; Jones, D. J.; Rozière, J. *Chem. Mater.* **1996**, *8*, 1758.

(8) (a) Guerrero-Ruiz, A.; Rodríguez-Ramos, I.; Fierro, J. L. G.; Jiménez-López, A.; Olivera-Pastor, P.; Maireles-Torres, P. *Appl. Catal. A* **1992**, *92*, 81. (b) Olivera-Pastor, P.; Rodríguez-Castellón, E.; Maza-Rodríguez, J.; Jiménez-López, A. *J. Mol. Catal. A* **1996**, *108*, 175. (c) De Stefanis, A.; Perez, G.; Ursini, O.; Tomlinson, A. A. G. *Appl. Catal. A* **1995**, *132*, 353.

(9) Cassagneau, T.; Hix, G.; Jones, D. J.; Maireles-Torres, P.; Rhomari, M.; Rozière, D. J. *J. Mater. Chem.* **1994**, *4*, 189.

(10) Maireles-Torres, P.; Olivera-Pastor, P.; Rodríguez-Castellón, E.; Jiménez-López, A.; Tomlinson, A. A. G. *J. Inclusion. Phenom.* **1992**, *14*, 327.

(11) Maireles-Torres, P.; Olivera-Pastor, P.; Rodríguez-Castellón, E.; Jiménez-López, A.; Tomlinson, A. A. G. In *Recent Developments in Ion Exchange 2*; Williams, P. A., Hudson, M. J., Eds.; Elsevier: London, 1990; p 95.

(12) Brousseau, L. C.; Aoki, K.; Garcia, M. E.; Cao, G.; Mallouk, T. E. In *Multifunctional Mesoporous Inorganic Solids*; Sequeira, C. A. C., Hudson, M. J., Eds.; NATO ASI, Kluwer Academic: Dordrecht, Germany, 1993; 400, 225−236.

(13) (a) Beck, J. S.; Vartuli, J. C.; Roth, W. J.; Leonowicz, M. E.; Kresge, C. T.; Schmitt, K. D.; Chu, C. T.-W.; Olson, D. H.; Sheppard, E. W.; McCullen, S. B.; Higgins, J. B.; Schlenker, J. L. *J. Am. Chem. Soc.* **1992**, *114*, 10834. (b) Chen, C. Y.; Li, H.-X.; Davis, M. E. *Microporous Mater.* **1993**, *2*, 17. (c) Ciesla, U.; Schacht, S.; Stucky, G. D.; Unger, K. K.; Schüth, F. *Angew. Chem., Int. Ed. Engl.* **1996**, *35*, 541. (d) Huo, Q.; Margolese, D. I.; Ciesla, U.; Feng, P.; Gier, T. E.; Sieger, P.; Leon, R.; Petroff, P. M.; Schüth, F.; Stucky, G. D. *Nature* **1994**, *368*, 317.

S0743-7463(96)01073-6 CCC: $14.00

phosphates,[13d] can be prepared by using an appropriate surfactant with an adequate concentration. Therefore, the way is now opened for the synthesis of highly expanded layered solids which, in turn, may be useful as starting materials for the preparation of other new compounds.

On the other hand, although the chemical similarities between Ga^{3+} and Al^{3+} are well-known,[14] relatively few studies about the influence of Ga^{3+} in nanostructured materials have been reported[15] until now. It has been demonstrated, for instance, that the introduction of gallium into silicates and aluminosilicates enhances the catalytic activity and selectivity toward the production of aromatic substances, which are of industrial importance.[16]

In this work, we report a sol−gel methodology for the synthesis of alkyltrimethylammonium−zirconium phosphate analogous to that used for MCM-type materials and the preparation of gallium oxide−zirconium phosphate composites from these precursors. The obtained materials have been characterized by X-ray diffraction (XRD), thermogravimetric analysis−differential thermal analysis (TGA-DTA), X-ray photoelectron spectroscopy (XPS), and N_2 adsorption−desorption at 77 K. Acid properties have been evaluated by thermal programmed desorption of ammonia (TPD-NH_3) and infrared (IR) study of adsorbed pyridine and the catalytic test of isopropyl alcohol decomposition.

Experimental Section

Direct Synthesis of Alkyltrimethylammonium−Zirconium Phosphate Intercalates. A new sol−gel method for the direct synthesis of alkyltrimethylammonium ($C_nH_{2n+1}N(CH_3)_3^+$, $n = 12$)−zirconium phosphate (C_{12}TMA-ZrP) materials has been developed in the present work. The synthesis was carried out by adding to different amounts of a surfactant, dodecyltrimethylammonium bromide, previously dissolved in 1-propanol, an orthophosphoric acid solution (85%), and zirconium tetra-*n*-propoxide 1-propanol solution, under vigorous stirring. In all cases the P:Zr molar ratio was 2, whereas the surfactant:Zr molar ratio was varied between 0.2 and 6. After 30 min, the resulting gel was separated by centrifugation, washed first with mixtures of *n*-propanol−water and then with distilled water up to pH 3, and finally air dried at 333 K.

Preparation of Gallium Oligomeric Solutions. A Ga^{3+} solution was obtained by dissolving metallic gallium (Strem Chemicals) with nitric acid under reflux for 1 day. After dilution with deionized water, the excess of nitric acid was removed by heating in a bath of sand, and the final concentration was adjusted to 0.7 M. This solution, with an initial pH of 1.8, was hydrolyzed by dropwise adding a 0.1 M *n*-propylamine aqueous solution up to a base:metal molar ratio of 2.5. The hydrolyzed solution with a final concentration of 0.04 M was finally aged at 323 K for 30 min and quickly cooled in an ice bath.[14b]

Insertion of Oligomeric Gallium Species into the Zirconium Phosphate Host. The intercalate with the highest loading of dodecyltrimethylammonium was chosen for inserting the oligomeric gallium species. A colloidal suspension of this intercalation compound (2 wt %) was put in contact with different volumes of the freshly prepared oligomeric gallium solution, stirred, and refluxed for 1 day. The resulting solids were then separated by centrifugation, washed off with distilled water, dried at room temperature (hereafter labeled as Ga-ZrP *x*, where *x* = added Ga:phosphate molar ratio), and finally calcined at 673 K for 4 h.

Characterization. Chemical analyses were carried out by atomic absorption spectroscopy (Zr and Ga), and P was determined colorimetrically. XRD was recorded on a Siemens D501 diffractometer using Cu Kα radiation and a graphite monochromator. TGA-DTA measurements were carried out under air using a Rigaku Thermoflex TG8110 instrument (calcined Al_2O_3 reference, 10 K min^{-1} heating rate). IR spectra were recorded with a Perkin Elmer 883 infrared spectrophotometer on KBr-diluted wafers.

The nitrogen adsorption−desorption isotherms at 77 K on calcined Ga-ZrP materials were obtained in a conventional volumetric apparatus, after outgassing of samples at 473 K and 10^{-4} Torr (overnight). Brunauer−Emmett−Teller (BET) specific surface areas were evaluated using 0.162 nm^2 as the cross-sectional area of the nitrogen-adsorbed molecule. Pore size distributions were calculated by the use of the Cranston and Inkley method for cylindrical pores.[17]

Samples for transmission electron microscopy (TEM) examination were prepared using an ultramicrotome to get thin sections of the selected materials that have been previously embedded in acrylic resin. Typical 75−100 nm thick specimens were then supported on copper electron microscope grids. Electron microscopy was carried out in a Philips CM 200 transmission electron microscope operated at 191 kV.

The X-ray photoelectron spectra were recorded with a Physical Electronics 5700 spectrometer equipped with a dual X-ray excitation source (Mg Kα, $h\nu = 1253.6$ eV, and Al Kα, $h\nu = 1486.6$ eV) and a multichannel hemispherical electron analyzer. The samples were turbopumped to ca. 10^{-9} Torr before they were moved into the analysis chamber. The residual pressure in this ion-pumped chamber was maintained below 10^{-9} Torr during data acquisition. The binding energies were obtained with an accuracy of ±0.1 eV and by charge referencing with the adventitious C 1s peak at 284.8 eV.

The total acidity of calcined Ga-ZrP materials was evaluated by TPD-NH_3. Before the adsorption of ammonia at 373 K, the samples were heated at 673 K in He flow. The TPD-NH_3 was carried out between 373 and 673 K, at 10 K min^{-1}, and analyzed by an on-line gas chromatograph (Shimadzu GC-14A) provided with a thermal conductivity detector.

Adsorption−desorption of pyridine was performed on self-supported wafers of calcined Ga-ZrP materials with weight-to-surface ratios of about 12 mg cm^{-2}. The wafers were placed in a vacuum cell assembled with greaseless stopcocks and CaF_2 windows. The samples were outgassed at 573 K under vacuum, before being exposed to pyridine vapor at room temperature. Desorption of pyridine was studied between room temperature and 623 K. IR spectra were recorded at room temperature using a Perkin Elmer 883 apparatus.

Calcined Ga-ZrP materials were also tested as catalysts for the reaction of the decomposition of isopropyl alcohol. A fixed-bed tubular glass working at atmospheric pressure was used for a catalyst charge of 30 mg without dilution. The isopropyl alcohol was fed into the reactor by bubbling a flow of He of 25 cm^3 min^{-1} through a saturator−condenser at 303 K, which allowed a constant isopropyl alcohol flow of 7.5 vol % and a spatial velocity of 46 μmol s^{-1} g^{-1}. Catalysts did not show diffusion restrictions. Prior to the catalytic test, the samples were pretreated at 593 K in a helium flow for 3 h. The reaction products were analyzed by an on-line gas chromatograph (Shimadzu GC-14A) provided with a flame ionization detector and a fused silica capillary column SPB1. The helium carrier was passed through a molecular sieve before it was saturated with isopropyl alcohol.

Results and Discussion

Characterization of Dodecyltrimethylammonium−Zirconium Phosphate Intercalates. The chemical analysis of the products obtained by the sol−gel method gave in all cases a P:Zr molar ratio very close to 2 and variable contents of surfactant and water (Table 1) according to the loading of surfactant in solution. The surfactant retention diagram is shown in Figure 1. Saturation is reached for C_{12}TMA:Zr molar ratios in solution higher than 3, which corresponds to a C_{12}TMA:Zr ratio of only 0.37 in the product. This value is

(14) (a) Bradley, S. M.; Kydd, R. A.; Yamdagni, R. *J. Chem. Soc., Dalton Trans.* **1990**, 413. (b) Bradley, S. M.; Kydd, R. A.; Yamdagni, R. *J. Chem. Soc., Dalton Trans.* **1990**, 2653. (c) Bradley, S. M.; Kydd, R. A.; Yamdagni, R. *Magn. Reson. Chem.* **1990**, *28*, 746. (d) Bradley, S. M.; Kydd, R. A.; Fyfe, C. A. *Inorg. Chem.* **1992**, *31*, 1181.

(15) (a) Kloprogge, J. T.; Booy, E.; Jansen, J. B. H.; Geus, J. W. *Clay Miner.* **1994**, *29*, 153. (b) Tang, X.; Xu, W. Q.; Shen, Y.-F.; Suib, S. L. *Chem. Mater.* **1995**, *7*, 102. (c) Bagshaw, S. A.; Cooney, R. P. *Chem. Mater.* **1995**, *7*, 1384. (d) Hernando, M. J.; Pesquera, C.; Blanco, C.; Benito, I.; González, F. *Chem. Mater.* **1996**, *8*, 76.

(16) Cheng, C. F.; He, H.; Zhou, W.; Klinowski, J.; Sousa-Gonçalves, J. A.; Gladden, L. F. *J. Phys. Chem.* **1996**, *100*, 390.

(17) Cranston, R. W.; Inkley, F. A. *Adv. Mater.* **1957**, *9*, 143.

Table 1. Chemical Compositions of Different Zirconium Phosphate Intercalates

sample	H_2O (%)	C_{12}TMA (%)	Ga (%)	empirical formulas[a]
C_{12}TMA-ZrP 0.2[b]	7.5	9.5		$ZrC_{12}TMA_{0.19}H_{1.81}(PO_4)_2 \cdot 1.9H_2O$
C_{12}TMA-ZrP 0.5[b]	8.0	12.7		$ZrC_{12}TMA_{0.25}H_{1.75}(PO_4)_2 \cdot 2.0H_2O$
C_{12}TMA-ZrP 2.0[b]	6.0	20.4		$ZrC_{12}TMA_{0.44}H_{1.56}(PO_4)_2 \cdot 1.6H_2O$
fresh Ga-ZrP 0.9	19.0	2.1	11.6	$Zr(Ga_{13})_{0.06}C_{12}TMA_{0.04}H_{1.54}(PO_4)_2 \cdot 4.5H_2O$
fresh Ga-ZrP 1.8	12.1	0.2	22.3	$Zr(Ga_{13})_{0.14}C_{12}TMA_{0.02}H_{1.00}(PO_4)_2 \cdot 3.7H_2O$
fresh Ga-ZrP 2.8	13.7	0.5	25.7	$Zr(Ga_{13})_{0.19}C_{12}TMA_{0.02}H_{0.65}(PO_4)_2 \cdot 5.1H_2O$
fresh Ga-ZrP 3.7	17.0	2.6	27.6	$Zr(Ga_{13})_{0.21}C_{12}TMA_{0.08}H_{0.45}(PO_4)_2 \cdot 7.8H_2O$

[a] Ga_{13}: $[GaO_4Ga_{12}(OH)_{12}(H_2O)_{24}]^{7+}$. [b] Numbers correspond to added C_{12}TMA:Zr ratio.

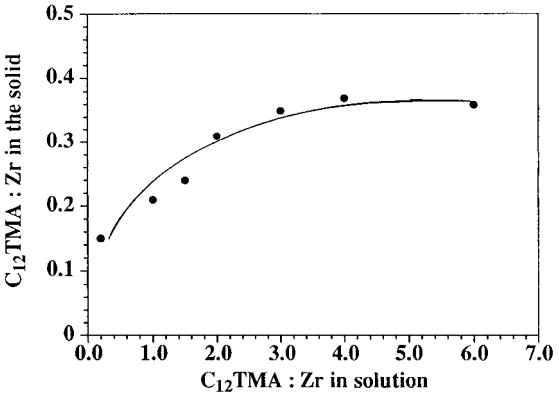

Figure 1. Retention diagram of dodecyltrimethylammonium (C_{12}TMA) into zirconium phosphate as a function of the initial C_{12}TMA:Zr ratio.

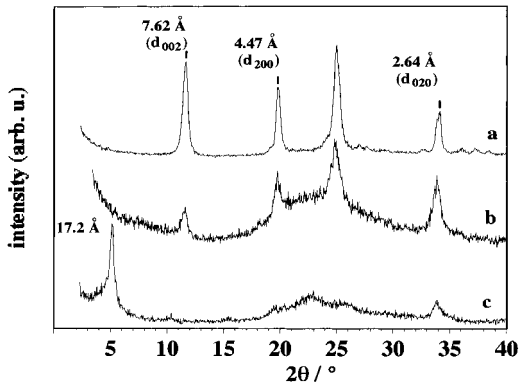

Figure 2. XRD patterns of (a) α-zirconium phosphate (α-ZrP), (b) C_{12}TMA-ZrP treated with 2 M orthophosphoric acid, and (c) sample b contacted with *n*-propylamine vapors.

approximately the half of that obtained when the surfactant is intercalated into colloidal *n*-propylamine−α-zirconium phosphate by ion exchange with *n*-propylammonium ions. Assuming that the thermodynamically most stable phase was formed (α-zirconium phosphate), the maximum retention of surfactant by the sol−gel method corresponds to a neutralization of about 19% of the acid groups of the phosphate. However, the assumption about the existence of a lamellar phase has to be argued. The first evidence is that α-zirconium phosphate (α-ZrP) is regenerated upon treatment with a 2 M orthophosphoric acid solution, as verified by the appearance of diffraction peaks at 7.62, 4.47, and 2.64 Å, characteristic of the α-ZrP (Figure 2). This regenerated α-ZrP swelled in the presence of *n*-propylamine showing a basal spacing of 17.16 Å and the characteristic reflections of the α layer structure at 4.36 and 2.65 Å (Figure 2). Noteworthy also is that the C_{12}TMA-ZrP phase calcined at 1273 K transforms into cubic zirconium pyrophosphate, a thermal behavior which would be expected for a layered structure.

The XRD study of the different C_{12}TMA-ZrP solids also reveals the presence of a diffraction peak at low angle which becomes more defined upon increasing the loading

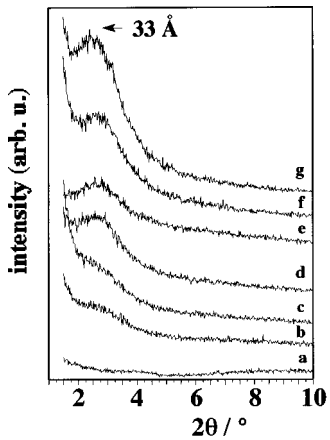

Figure 3. XRD patterns of C_{12}TMA-ZrP at different surfactant: zirconium ratios: (a) 0.2, (b) 1.0, (c) 1.5, (d) 2, (e) 3, (f) 4.0, and (g) 6.0.

Scheme 1

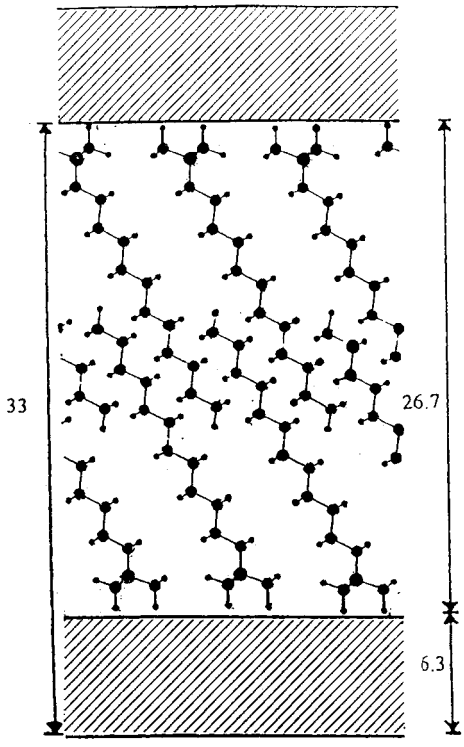

of C_{12}TMA (Figure 3). This peak, at 33 Å, may be attributed to the basal spacing in a lamellar system. If the α-type structure with a layer thickness of 6.3 Å[18] is assumed, a bilayer arrangement of the surfactant cation in the interlayer region could be feasible, taking into account that its dimensions are 19.3 Å of length and 55 $Å^2$ of cross section for the polar head. With this arrangement the tetraalkylammonium ions would be oriented in a slanted position with respect to the layer of 65° and

(18) Alberti, G.; Costantino, U. In *Intercalation Chemistry*; Withingham, M. S., Ed.; Academic Press: New York, 1982; p 147.

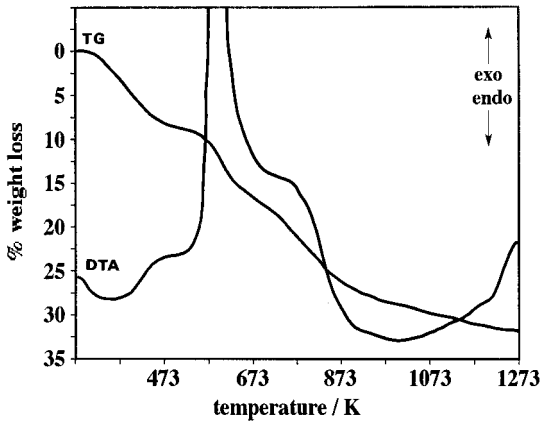

Figure 4. Typical thermogravimetric curves (TGA-DTA) of C_{12}TMA-ZrP.

partially imbricated to one another 5.9 Å (Scheme 1). The absence of peaks corresponding to other *hkl* reflections is due to the low crystallinity of the synthesized host material, which in turn will be an advantage from the catalytic viewpoint (*vide infra*).

Thermal analyses of the C_{12}TMA-ZrP intercalates (Figure 4) provide additional proofs about the layered nature of these materials. The fact that the organic matter is removed at high temperature (exothermic effects in the DTA curves between 600 and 823 K) is attributed to the existence of a strong interaction between the alkyl chains and is characteristic of an arrangement of organic molecules closely packed in the interlayer region of a layered solid. The partial carbonization of the organic matter, observed in other layered phases[13c] as well and detected by the black color of the residue obtained at 1273 K, also supports this assumption. In an organic−inorganic system other than a lamellar phase, elimination of the organic matter would be expected to occur at lower temperatures due to a less effective interaction between the alkyl chains. Percentages of organic matter range between 8.5 and 21.5 wt % and the water content between 5.6 and 8.0 wt %. The removing of adsorbed water is associated with an endothermic effect near 373 K.

Characterization of Gallium-Exchanged Zirconium Phosphate Materials. Although Ga^{3+} is more acidic than Al^{3+}, the hydrolytic behavior of both cations is quite similar. This has been confirmed by the work of Bradley et al.,[14b] who have reported the existence of an oligomeric species of Ga^{3+} similar to the tridecameric ion $[AlO_4(OH)_{24}(H_2O)_{12}]^{7+}$, in short Al_{13}. These authors could obtain an oligomeric Ga^{3+}-intercalated phase of montmorillonite with an interlayer distance very close to that expected for an intercalated Ga_{13} species $[GaO_4Ga_{12}(OH)_{12}(H_2O)_{24}]^{7+}$. In this work an oligomeric Ga^{3+} solution has been prepared following closely the experimental conditions used by Bradley et al.,[14b] except that *n*-propylamine was added instead of NaOH in order to avoid the effects of ion competition.

A saturated C_{12}TMA-ZrP phase was employed as exchanger, and the Ga:phosphate molar ratio was varied between 0.9 and 3.7 in order to study the influence of the gallium loading on the resulting solids. Table 1 displays the chemical composition of Ga-ZrP materials. After exchange with oligomeric Ga^{3+}, the surfactant was present only as a residue in all samples. The uptake of gallium by the phosphate shows a tendency to the formation of saturated phases, but additions of gallium with ratios higher than 4.0 lead to the precipitation of gallium oxohydroxide outside the interlayer region, which is observed in the XRD diagrams by the appearance of peaks characteristic of this compound at 4.09, 2.61, and 2.37 Å. Assuming that the Ga_{13} species was intercalated, the maximum amount taken up was 0.21 mol of Ga_{13} per mol of exchanger.

Figure 5. Typical TEM micrographs of Ga-ZrP 2.8 calcined at 673 K.

The X-ray diffraction patterns of both fresh and calcined Ga-ZrP materials did not exhibit any diffraction peak. This might be expected, taking into account the low degree of crystallinity of the intermediate C_{12}TMA-ZrP used to insert the Ga polyoxycations and that this intermediate was completely delaminated in water before contact with the oligomeric Ga^{3+} solution. However, complete disruption of the phosphate layer structure would not be expected to occur during the mild exchange reaction conditions. TEM micrographs (Figure 5) point to the lamellar nature maintained in Ga-ZrP materials, although in no case long-range order of the layer packets could be detected by XRD. A complex pattern with peaks corresponding to tetragonal zirconium oxide and gallium phosphate was obtained after calcination at 1273 K. This thermal behavior is similar to that observed with crystalline layered Al-ZrP materials calcined at the same temperature[5b] but different from that of the C_{12}TMA-ZrP intercalate which is instead transformed to cubic zirconium pyrophosphate. Therefore, the presence of intercalated gallium oxo-species, like the aluminum ones, strongly bonded to the phosphate groups preclude the pyrophosphate formation and lead to the destruction of the host structure at temperatures so high as 1273 K. Moreover, the systematic absence, in all cases, of diffraction peaks corresponding to gallium oxohydroxide or gallium oxide, throughout the range of temperature studied, rules out the presence of these substances outside the phosphate host.

Surface Properties of Calcined Ga-ZrP Materials. XPS provides valuable information about the surface composition. A comparison of the bulk and surface Ga:Zr atomic ratios (Figure 6) for calcined solids indicates that the materials are indeed homogeneous phases, as these ratios matched very well for all samples. On the other hand, the binding energies (BE) of Ga 2p for the calcined solids (1117.6−1118.2 eV) is higher than that of the pure gallium oxide (1117.3 eV) and, therefore, suggest a strong interaction of gallium oxide with the phosphate layers; in addition these values are not consistent with the presence

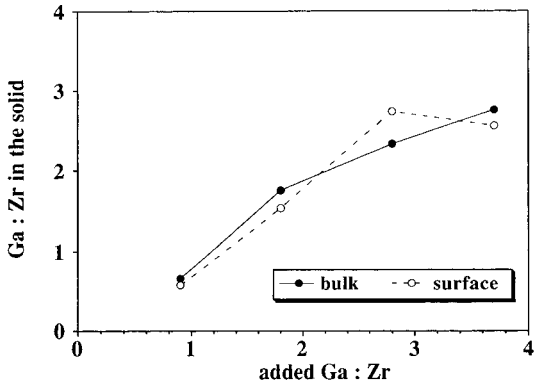

Figure 6. Bulk and surface (XPS) Ga:Zr ratio in calcined Ga-ZrP materials as a function of the added Ga:Zr ratios.

Table 2. Core Level Binding Energies (eV) Measured for Calcined Ga-ZrP Materials, α-ZrP, and Ga_2O_3

sample	Zr $3d_{5/2}$ BE (eV)	P 2p BE (eV)	Ga $2p_{3/2}$ BE (eV)
Ga-ZrP 0.9	183.3	134.1	1118.2
Ga-ZrP 1.8	183.1	133.7	1117.7
Ga-ZrP 2.8	182.9	133.8	1117.6
Ga-ZrP 3.7	182.5	133.3	1117.6
α-ZrP	183.7	134.2	
Ga_2O_3			1117.3

Table 3. Textural Parameters of Ga-ZrP Samples Calcined at 673 K

sample	S_{BET} ($m^2\ g^{-1}$)	V_p[a] ($cm^3\ g^{-1}$)	S_{ext}[b] ($m^2\ g^{-1}$)	ΣV_p[b] ($cm^3\ g^{-1}$)	d_p (m)[b] (Å)	V_{micro}[c] ($cm^3\ g^{-1}$)
Ga-ZrP 0.9	340	0.352	377	0.333	35	0.143
Ga-ZrP 1.8	343	0.495	392	0.484	49	0.135
Ga-ZrP 2.8	295	0.546	355	0.506	57	0.117
Ga-ZrP 3.7	366	0.515	439	0.438	40	0.141

[a] At $P/P° = 0.98$. [b] Accumulated surface and pore volume as calculated by the Cranston and Inkley method. [c] Using the Dubinin−Radushkevich equation.

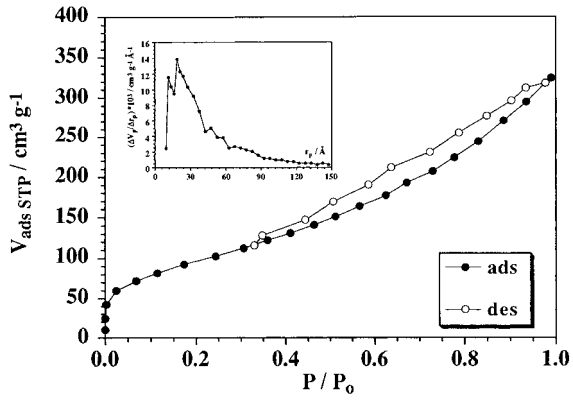

Figure 7. Adsorption−desorption isotherms of N_2 at 77 K and pore size distribution (inset) of calcined Ga-ZrP 1.8 sample.

of segregated gallium oxide. All the other chemical elements (P, Zr, and O) show nearly constant BE throughout the series of precursor and calcined solids (Table 2), and these are similar to those presented by analogous intercalated zirconium phosphate materials.[4]

Textural parameters of calcined Ga-ZrP materials are summarized in Table 3. N_2 adsorption−desorption isotherms at 77 K (Type IV in the IUPAC clasification[19]) are typical of mesoporous solids (Figure 7), but the initial adsorption at low relative pressure is also indicative of the existence of micropores, as revealed by using the

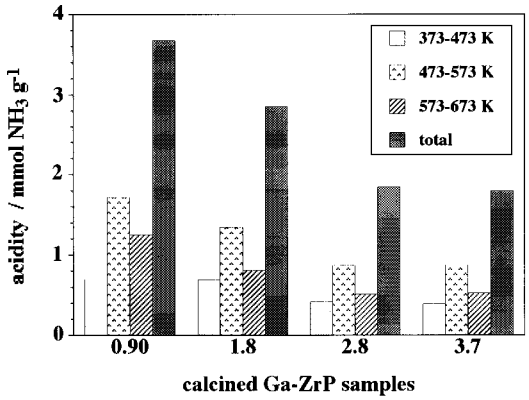

Figure 8. Total acidity of calcined Ga-ZrP materials from TPD-NH_3.

Dubinin−Radushkevich equation.[20] The values of micropore volume ranged between 0.117 and 0.143 $cm^3\ g^{-1}$ which corresponds to 20−40% of the total pore volume. These micropores might be generated by a pillaring process of the host with nanoparticles of gallium oxide. BET surface areas (295 and 366 $m^2\ g^{-1}$) seem to be independent of the Ga content and are much higher (10-fold) than those which could correspond to a hypothetical mixture of gallium oxide and zirconium phosphate, taking into consideration the low surface areas of these two materials (51 and 22 $m^2\ g^{-1}$, respectively). All calcined materials exhibit narrow pore size distributions (Figure 7) (Cranston and Inkley method based on a cylindrical model of pores), the larger of those being Ga-ZrP 1.8 and Ga-ZrP 2.8 which could be interesting for catalytic purposes. These materials show pore size distributions with most of pore radii comprised between 15 and 60 Å. It is generally assumed that a high contribution of micropores is a typical feature of pillared layered structures, whereas the mesopores stem in great part from cavities formed by packets of layers as a consequence of end−end and end−edge interactions.

Standard techniques such as thermal programmed desorption of ammonia and infrared spectroscopy of samples with adsorbed pyridine have been employed for the acid characterization of the calcined Ga-ZrP materials. TPD-NH_3 provides a quantitative estimation of the total number of acid sites and the distribution of acid strengths, while the IR study of adsorbed pyridine is helpful to monitor the Lewis and Brønsted acidity. Both methods show the remarkable acidity of these materials, which is comparable with that of many zeolites.[1] TPD-NH_3 curves do not show bands clearly defined, indicating a broad distribution of acid strengths. Moreover, after outgassing at temperatures as high as 673 K, there is still a residue of adsorbed ammonia (as revealed by IR spectroscopy), which may be indicative of the presence of very strong acid sites. Figure 8 displays the variation of the total acidity with the temperature for the Ga-ZrP composites. The acidity values range between 1.8 and 3.7 mmol of $NH_3\ g^{-1}$, being even higher than those reported for others pillared layered zirconium phosphate materials.[9b] The total acidity decreases with the gallium content, similarly as in aluminium oxide pillared zirconium phosphate samples, and this trend can be explained by a progressive decrease in the number of accessible Brønsted acid sites associated to P−OH groups. As can be seen in Figure 8, a high proportion of ammonia is desorbed between 473 and 573 K, which seems an optimal range for the use of these materials as acid catalysts.

The IR spectra in the region 1400−1700 cm^{-1} of samples with adsorbed pyridine (Figure 9) show the presence of both Brønsted and Lewis acid sites at 1550 cm^{-1} and 1450 cm^{-1}, respectively. Extinction coefficient values of 1.11 and 0.73 cm μmol^{-1} for Brønsted and Lewis acid vibration

(19) Sing, K. S. W.; Everett, D. H.; Haul, R. A. W.; Moscou, L.; Pierotti, R. A.; Rouquerol, J.; Siemieniewska, T. *Pure Appl. Chem.* **1985**, *57*, 603.
(20) Gregg, S. J.; Sing, K. S. W. *Adsorption Surface Area and Porosity*, 2nd ed.; Academic Press: New York, 1982; p 221.

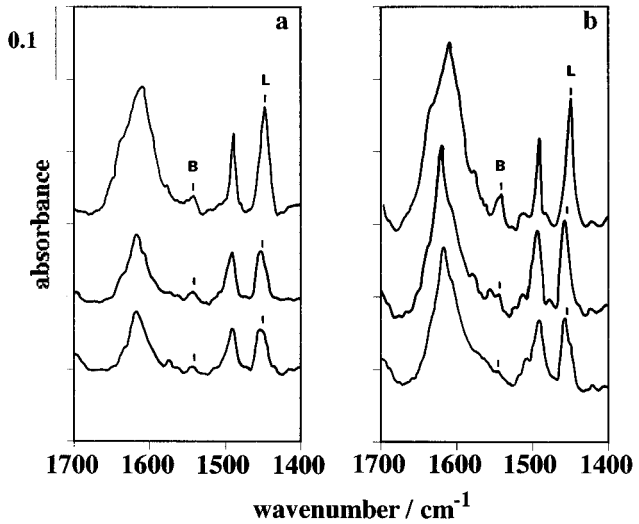

Figure 9. IR spectra of (a) calcined Ga-ZrP 1.8 and (b) calcined Ga-ZrP 3.7, exposed to pyridine vapors and outgassed at different temperatures.

Table 4. Percentages of Lewis Acid Sites (% L) in Ga-ZrP Materials, Calcined at 673 K, As Determined by Pyridine Adsorption, Outgassed at Different Temperatures

	% L		
material	293 K	493 K	623 K
Ga-ZrP 0.9	76	58	100
Ga-ZrP 1.8	86	79	86
Ga-ZrP 2.8	83	96	100
Ga-ZrP 3.7	88	100	100

bands[21] were used in order to determine the percentages of Brønsted and Lewis acid sites at different outgassing temperatures (Table 4). A higher concentration of Lewis sites was found for all samples at 293 K. Furthermore, the percentage of Lewis acid sites which remained bonded to pyridine upon raising the outgassing temperature up to 623 K was close to 100%. This indicates that a significant fraction of the Lewis acid sites are stronger than those of Brønsted-type. The Lewis acidity is probably associated to gallium ions with low coordination, whereas the Brønsted acidity could be due to acid OH groups from the host and the intercalated Ga(III) species. IR spectra were recorded for calcined Ga-ZrP samples before and after adsorption of these basic molecules but unfortunately the vibration bands were too broad, and hence a discrimination of the different kinds of OH groups present in these materials was not possible. In any case, no appreciable changes in the characteristic structural bands of calcined Ga-ZrP materials were observed upon adsorption−desorption of ammonia or pyridine.

The decomposition of isopropyl alcohol has been chosen as a test reaction in order to evaluate the acidic nature of the active sites. It is well-established that acid sites produce propene (dehydration reaction), whereas basic and redox sites are responsible for the production of acetone (dehydrogenation reaction). Calculated activation energy values were in the range 113−132 kJ mol^{-1}, suggesting that this catalytic reaction was not controlled by diffusion of the isopropyl alcohol molecules.[22]

(21) Datka, J.; Turek, A. M.; Jehng, J. M.; Wachs, I. E. *J. Catal.* **1992**, *135*, 186.

(22) Bond, G. C. *Heterogeneous Catalysis. Principles and Applications*, 2nd ed.; Clarendon Press: Oxford, 1987.

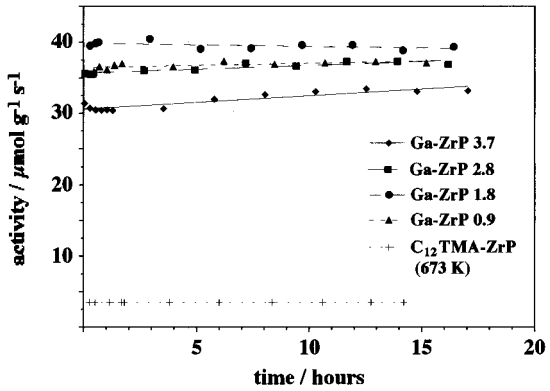

Figure 10. Catalytic activity of calcined Ga-ZrP materials for the decomposition of isopropyl alcohol as a function of time on stream.

Calcined Ga-ZrP materials show very high activities (Figure 10) with values comprised between 30 and 40 μmol g^{-1} s^{-1}, conversions close to 100%, and a total selectivity toward propene. This activity probably arises from the high concentration of acid sites of moderate strength present in these porous materials, as revealed by TPD-NH_3 and pyridine adsorption. Thus, the less acidic sample (Ga-ZrP 3.7) displays the lowest activity. The other three samples show a similar behavior in spite of their different total acidity, indicating that the accessibility of the isopropyl alcohol molecules to internal pores may be an important factor controlling the activity of these materials. In any case, the catalytic activity is maintained almost unchanged after 18 h on stream. On the contrary, the dodecyltrimethylammonium−zirconium phosphate intercalate, calcined at 673 K, displayed very low catalyic activity (3.5 μmol g^{-1} s^{-1}) probably due to majority of the active sites (situated in the interlayer phosphate region) were innaccessible to reactant molecules by total or partial collapse of the interlayer region after removing the organic matter. Furthermore, the precipitate obtained by adding an excess of *n*-propylamine to a Ga(III) oligomeric solution and calcined at 400 °C (α-Ga_2O_3) did not show any appreciable activity under the same experimental conditions.

Conclusions

Layered dodecyltrimethylammonium−zirconium phosphate intercalates have been directly synthesized by using a sol−gel methodology at room temperature. The surfactant molecules tend to arrange closely packed into the interlayer region forming a bilayer. These intercalates colloidized well in water and easily exchanged the organic cation with bulky inorganic species, such as gallium oligomeric cations.

Ga(III) zirconium phosphate materials calcined at 673 K were highly porous solids with microporosity and mesoporosity and a remarkable acidity, mainly Lewis type. The use of the test reaction of isopropyl alcohol decomposition has revealed the high catalytic activity of these materials, which show, at 493 K, conversions close to 100% and a total selectivity toward propene.

Acknowledgment. This research was supported by the CICYT (Spain) Project MAT 94-0678 and CE Programme BRITE-EURAM Contract BRE-CT93-0450. J.J.J. thanks the Junta de Andalucía for a fellowship.

LA961073S